AIAA JOURNAL
Vol. 43, No. 2, February 2005

Verification and Validation of Time-Domain Impedance Boundary Condition in Lined Ducts

Shi Zheng* and Mei Zhuang†
Michigan State University, East Lansing, Michigan 48824

A computational-aeroacoustics (CAA) code in the time domain has been developed for duct acoustics problems. A time-domain broadband impedance boundary condition is implemented in the code to simulate the acoustic liner. To verify the boundary condition in a duct environment, the CAA code is used to solve a semi-infinite two-dimensional duct problem with an acoustic liner for cases both with and without a sheared mean flow. The results from the numerical prediction tool agree excellently with the analytic solutions. In addition, the CAA code is validated by the experimental data from the NASA Langley Research Center flow impedance tube facility. It predicts accurately both the amplitude and the phase of the sound propagation from the NASA experiment. In both the verification and the validation problems, the no-slip condition is assumed for the mean flow to avoid the controversy over the condition of particle displacement continuity and the condition of particle velocity continuity and also to ensure the well-posedness of a time-domain broadband impedance boundary condition.

Nomenclature

C	=	constant
c_0	=	velocity scale, 344 m/s
f	=	frequency
h	=	duct height
Im	=	imaginary part
k_x, k_y	=	x and y components of wave number
L	=	length scale, 1 m
M	=	mean flow Mach number in the x direction
p	=	acoustic pressure
$\hat{p}$	=	time-harmonic acoustic pressure
R	=	specific resistance
R_0, X_{-1}, X_1	=	parameters of the three-parameter impedance model
Re	=	real part
t	=	time
u, v	=	acoustic velocities in the x and y directions, respectively
v_n	=	acoustic normal velocity (positive when pointing into the treatment from the fluid side)
$\hat{v}_n$	=	time-harmonic acoustic normal velocity (positive when pointing into the treatment from the fluid side)
X	=	specific reactance
x, y	=	Cartesian coordinates
Z	=	specific impedance
γ	=	ratio of specific heats
Δt	=	time step
Δx, Δy	=	grid sizes in the x and y directions, respectively
ρ	=	acoustic density
ρ_0	=	density scale, 1.29 kg/m^3
σ_x	=	absorption coefficient for the perfectly matched layers boundary condition
Φ, U, V, P	=	complex-numbered y dependence of ρ, u, v, and p
φ	=	phase
ω	=	angular frequency, also wave number for the nondimensional case

Subscripts and Superscripts

in	=	incoming wave
$'$	=	first derivative with respect to y
$''$	=	second derivative with respect to y

I. Introduction

NOISE, as an environmental issue, has a major impact on both the conceptual and detailed design of the modern aircraft engine. Because of the large bypass ratios in modern aircraft engines, fan noise is becoming an increasingly important noise source during the critical takeoff and landing phases. Novel acoustic liners designed to attenuate such noise are therefore vital for the noise reduction of modern aircraft turbofan engines. These designs usually rely on extensive experimental tests, which are very expensive and time consuming. To achieve optimal acoustic liner designs, it is necessary to have accurate impedance models and aeroacoustic prediction tools so that acoustic fields inside and radiated from both inlet and exhaust of turbofan engines can be predicted accurately and efficiently. For this reason, there have been ongoing research activities for the development of numerical noise prediction systems[1–14] and impedance boundary conditions.[15–24]

To take advantages of the recent development of computational aeroacoustics (CAA), time-domain simulations, which require time-domain impedance boundary conditions in predicting noise generation and propagation in duct acoustics, have been exploited in the past few years. Because the liner impedance is conventionally defined in the frequency domain, such information must be properly converted into the time domain to serve as a well-posed boundary condition for the governing equations. Tam and Auriault developed their time-domain single-frequency and broadband impedance boundary conditions for the three-parameter impedance model of the Helmholtz resonator type, by implicitly using the derivative properties of the Fourier transform.[17] Özyörük and Long borrowed the idea from the computational electromagnetics community and proposed their time-domain surface acoustic impedance condition based on the z transform.[18] Fung and Ju applied the inverse Fourier transform to the reflection coefficient instead of the corresponding impedance, resulting in a stable time-domain impedance boundary condition.[19,20]

Received 20 December 2003; revision received 9 June 2004; accepted for publication 30 August 2004.

*Graduate Research Assistant, Department of Mechanical Engineering. Student Member AIAA.

†Associate Professor, Department of Mechanical Engineering; zhuangm@egr.msu.edu. Senior Member AIAA.

Up to now, Özyörük et al.,[21] Özyörük and Long,[22] and Ju and Fung[23] have applied their own time-domain impedance boundary conditions to the NASA Langley flow impedance tube, for which experimental data are available. Favorable predictions of the sound pressure level (SPL) were reported for the both groups, but predictions of the phase information have not been published. Tam and Auriault have tested their time-domain impedance boundary condition for one-dimensional problem.[17] In our previous work,[24] the accuracy and effectiveness of their broadband time-domain impedance boundary condition have been verified for a three-dimensional acoustic problem with an acoustically treated boundary. Because of the difference in geometry between a duct and an open space, which results in the concept of modes for a duct configuration, it is necessary to further verify and validate the time-domain broadband impedance boundary condition in a duct configuration before a further development of a noise prediction tool for turbofan engine inlet ducts and turbomachinary using time-domain CAA methods. This validation is the primary objective of the current study.

In Sec. II, a semi-infinite impedance duct problem is proposed, and its analytical solution is given. In addition the numerical scheme is introduced along with the time-domain broadband impedance boundary condition and other relevant types of boundary conditions. The numerical results are compared with those of the analytical solution at the end of the section. In Sec. III, the configuration of the NASA Langley flow impedance tube facility is introduced, for which the numerical method is again implemented, and the results are compared with the experimental data. The effects of the exit boundary condition are also discussed. The conclusions are drawn in Sec. IV.

Unless otherwise stated, variables used in this paper are dimensionless with L/c_0 as the timescale, $\rho_0 c_0^2$ as the pressure scale, and $\rho_0 c_0$ as the impedance scale. The harmonic time dependence $\exp(i\omega t)$ is assumed. Under this convention, the impedance is $Z = R + iX$.

II. Verification with Analytical Solution

A. Verification Problem and Its Analytical Solution

To verify the time-domain impedance boundary condition, we consider a semi-infinite two-dimensional duct with a hard upper wall and an acoustically treated lower wall. The lower wall is characterized by its frequency-dependent impedance defined as

$$Z(\omega) = \hat{p}(\omega)/\hat{v}_n(\omega) \tag{1}$$

The mean flow velocity inside the duct is parallel in the x direction, that is, $M_x = M(y)$ and $M_y = 0$. The mean flow density and pressure are constant and equal to ρ_0 and $\rho_0 c_0^2/\gamma$, respectively. Such a duct configuration is shown in Fig. 1. The orientation of the coordinate system is as shown in the figure, and its origin is at the lower left corner of the duct.

This problem is governed by the two-dimensional linearized Euler equations (LEE) with a parallel mean flow in the x direction:

$$\frac{\partial \boldsymbol{u}}{\partial t} + \boldsymbol{A}\frac{\partial \boldsymbol{u}}{\partial x} + \boldsymbol{B}\frac{\partial \boldsymbol{u}}{\partial y} + \boldsymbol{D}\boldsymbol{u} = 0 \tag{2}$$

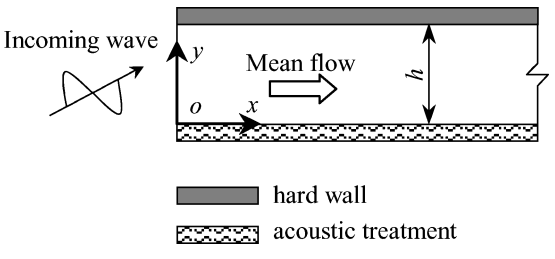

Fig. 1 Semi-infinite impedance duct.

where

$$\boldsymbol{u} = \begin{bmatrix} \rho \\ u \\ v \\ p \end{bmatrix}, \qquad \boldsymbol{A} = \begin{bmatrix} M(y) & 1 & 0 & 0 \\ 0 & M(y) & 0 & 1 \\ 0 & 0 & M(y) & 0 \\ 0 & 1 & 0 & M(y) \end{bmatrix}$$

$$\boldsymbol{B} = \begin{bmatrix} 0 & 0 & 1 & 0 \\ 0 & 0 & 0 & 0 \\ 0 & 0 & 0 & 1 \\ 0 & 0 & 1 & 0 \end{bmatrix}, \qquad \boldsymbol{D} = \begin{bmatrix} 0 & 0 & 0 & 0 \\ 0 & 0 & M'(y) & 0 \\ 0 & 0 & 0 & 0 \\ 0 & 0 & 0 & 0 \end{bmatrix}$$

When the solution to the LEE is assumed to have the form

$$\boldsymbol{u} = \begin{bmatrix} \Phi(y) \\ U(y) \\ V(y) \\ P(y) \end{bmatrix} \exp[i(\omega t - k_x x)] \tag{3}$$

Eq. (2) can be reduced to a second-order ordinary differential equation for $P(y)$ only:

$$P'' + \frac{2k_x}{\omega - M(y)k_x} M'(y) P' + \left\{ [\omega - M(y)k_x]^2 - k_x^2 \right\} P = 0 \tag{4}$$

At the upper boundary of the duct, the boundary condition is given as the hard wall boundary condition

$$P'(h) = 0 \tag{5}$$

To give the boundary condition at the acoustic treatment, we have to face a controversy as to whether the condition of particle displacement continuity (PDC) or the condition of particle velocity continuity (PVC) is to be used. When PDC or PVC is satisfied, the boundary condition at the lower boundary at $y = 0$ is

$$Z\omega P' + i[\omega - M(0)k_x]^2 P = 0 \tag{6}$$

or

$$ZP' + i[\omega - M(0)k_x]P = 0 \tag{7}$$

It is not an intention of this paper to solve such a controversy. However, if no-slip condition is assumed, for example, the mean flow is zero, at the acoustic treatment, it is easy to verify that Eq. (6) is the same as Eq. (7), and thus the controversy is avoided. On the other hand, if slip condition is assumed instead, the boundary condition (6) or its time-domain equivalents will lead to an unstable solution and thus is ill posed. Any time-domain solution with such a boundary condition is prone to stability problems.[17,25] Although the stability analysis was done in a semi-infinite domain, our numerical results show stability problems even in a duct configuration. For these reasons, the no-slip condition is assumed in the current study. For such a case, both Eqs. (6) and (7) are reduced to

$$ZP' + i\omega P = 0 \tag{8}$$

Equations (4), (5), and (8) define an eigenvalue problem with k_x being the eigenvalue. For a general sheared mean flow profile $M(y)$, the problem is not analytically solvable, and thus numerical procedure must be employed. For the zero mean flow case, the solution (for the right propagating wave) can be given as

$$P(y) = C\cos[k_y(h - y)] \tag{9}$$

where constant C is resulted from solving the eigenvalue problem; k_y is determined by solving the following transcendental equation:

$$Zk_y \tan(k_y h) - i\omega = 0 \tag{10}$$

with

$$k_x = \sqrt{\omega^2 - k_y^2} \tag{11}$$

The eigenvalue problem has a series of eigenvalues k_x, each corresponding to a mode allowed in such a duct configuration. We have calculated the least attenuated mode allowed in the configuration shown in Fig. 1 with duct width $h = 0.0508$, test frequency $2000L/c_0$, and specific impedance $Z = 4.99 + 0.25i$ for the treatment. For the zero mean flow case, $k_x = 36.2 - 1.94i$, $k_y = 9.13 + 7.67i$, and $P(y)$ is given by Eq. (9). For the case with a sheared mean flow $M(y) = 1.2(y/h)(1 - y/h)$ of centerline Mach number $M(h/2) = 0.3$, $k_x = 30.0 - 1.36i$, and $P(y)$ is obtained by numerically solving Eqs. (4), (5), and (8). These two cases will serve as test cases to verify our numerical methods in Sec. II.C.

Once $P(y)$ is known, the solution to the LEE in Eq. (2) can be determined by using Eq. (3) and the following equation:

$$\Phi(y) = \frac{k_x U(y) + iV'(y)}{\omega - M(y)k_x}$$

$$U(y) = \frac{k_x}{\omega - M(y)k_x} P(y) - \frac{M'(y)}{[\omega - M(y)k_x]^2} P'(y)$$

$$V(y) = \frac{i}{\omega - M(y)k_x} P'(y) \tag{12}$$

When presenting the calculated results later in Sec. II.C, we will use the SPL(x) and the phase relative to point at $(0, h)$ along the upper wall. From Eq. (3),

$$\mathrm{SPL}(x) - \mathrm{SPL}(0) = 20(\log_{10} e)\mathrm{Im}(k_x)x \tag{13}$$

where the sound pressure level at the inlet SPL(0) is determined by the reference pressure. The phase relative to the phase at point $(0, h)$ is

$$\varphi(x) = -\mathrm{Re}(k_x)x \tag{14}$$

B. Methodology of the Numerical Implementation

1. Inlet and Exit Boundary Conditions

When we numerically solve the semi-infinite impedance duct problem, the computational domain can only be a segment of the duct, starting at $x = 0$ and ending at some $x > 0$. To simulate the infinite extension to the right of the duct, it is required that all of the outgoing waves leave the computational domain without being reflected at the artificial duct exit. The same requirement applies for the duct inlet at $x = 0$, and, additionally, the incoming wave in Eq. (3) should be specified. For these purposes, we implement the perfectly matched layers (PML) boundary conditions in unsplit physical variables[26] in vertical x layers (PML regions) left to the inlet and right to the exit:

$$\frac{\partial \boldsymbol{u}'}{\partial t} + \boldsymbol{A}\frac{\partial \boldsymbol{u}'}{\partial x} + \boldsymbol{B}\frac{\partial \boldsymbol{u}'}{\partial y} + \boldsymbol{D}\boldsymbol{u}' + \sigma_x \boldsymbol{B}\frac{\partial \boldsymbol{q}}{\partial y}$$

$$+ \sigma_x \boldsymbol{u}' + \frac{\sigma_x M(y)}{1 - M^2(y)}\boldsymbol{A}\boldsymbol{u}' = 0 \tag{15}$$

where $\boldsymbol{u}' = \boldsymbol{u} - \boldsymbol{u}_{\mathrm{in}}$, with $\boldsymbol{u}_{\mathrm{in}}$ being the incoming wave specified in Eq. (3), for the inlet boundary condition, and $\boldsymbol{u}' = \boldsymbol{u}$ for the outlet boundary condition. And $\boldsymbol{q}$ is an auxiliary variable and is defined by

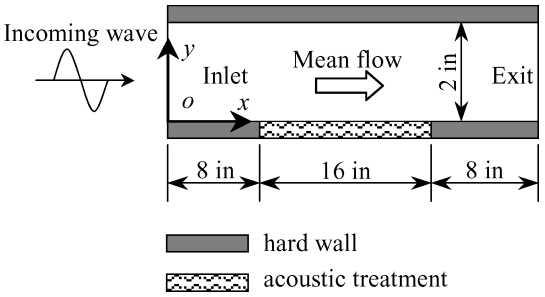

Fig. 4 Configuration of the NASA Langley flow impedance tube.

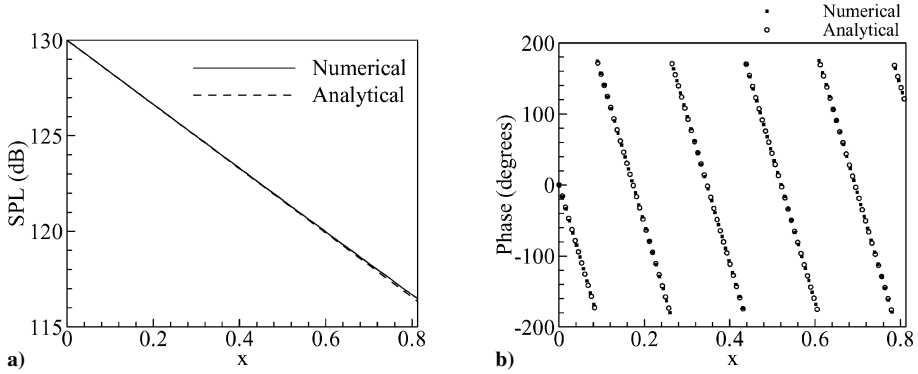

Fig. 2 Comparison of the numerical solution with the analytical solution for the least attenuated mode of the semi-infinite duct problem with a zero mean flow: a) sound pressure level along the hard wall and b) phase along the hard wall.

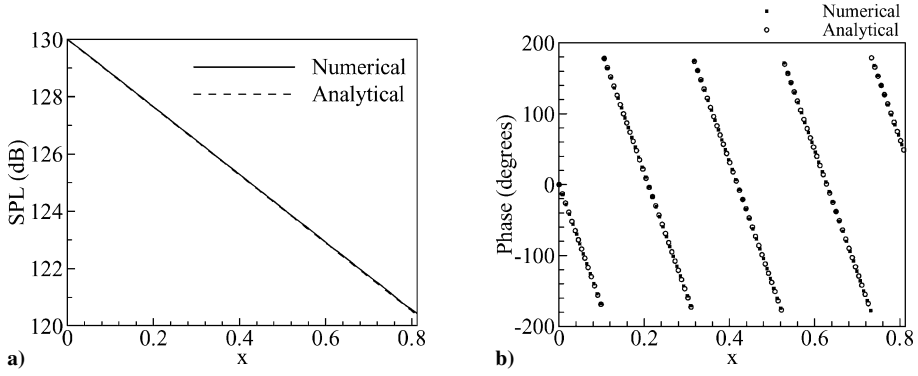

Fig. 3 Comparison of the numerical solution with the analytical solution for the least attenuated mode of the semi-infinite duct problem with a sheared mean flow $M(y) = 1.2(y/h)(1-y/h)$: a) sound pressure level along the hard wall and b) phase along the hard wall.

$\partial \boldsymbol{q}/\partial t = \boldsymbol{u}'$; σ_x spatially varies and takes the same form as in Ref. 26. At the outer boundaries of the PML regions, a characteristics-based boundary condition is applied to further improve the quality of the absorbing boundary conditions.

We need to point out that in Ref. 26 the PML boundary condition is proposed for a uniform mean flow, and its well posedness is only proved in the same context. In spite of this, our numerical solution as seen later shows the success of the boundary condition for a nonuniform flow.

2. Impedance Boundary Condition

At the acoustically treated wall, the broadband time-domain impedance boundary condition proposed by Tam and Auriault[17] is applied:

$$\frac{\partial p}{\partial t} = R_0 \frac{\partial v_n}{\partial t} - X_{-1} v_n + X_1 \frac{\partial^2 v_n}{\partial t^2} \tag{16}$$

where R_0, X_{-1}, and X_1 are related to the impedance by $R(\omega) = R_0$ and $X(\omega) = X_{-1}/\omega + X_1 \omega$.

Equation (16) is valid only when the no-slip condition is satisfied at the acoustic treatment. For the slip condition and also PDC to be satisfied, a time-domain impedance boundary condition similar to Eq. (16) can be found to be

$$\frac{\partial p}{\partial t} + M \frac{\partial p}{\partial x} = R_0 \frac{\partial v_n}{\partial t} - X_{-1} v_n + X_1 \frac{\partial^2 v_n}{\partial t^2} \tag{17}$$

However this boundary condition has been found to be unstable both analytically and by our numerical experiments, a result supporting the analysis in Refs. 17 and 25.

The stability analysis in Refs. 17 and 25 shows that time-domain impedance boundary conditions are unstable with the combination of PDC and slip condition. This limitation is not unique to the current time-domain formulation in Eq. (17). It is a challenge to be overcome for any time-domain impedance boundary conditions. However, we

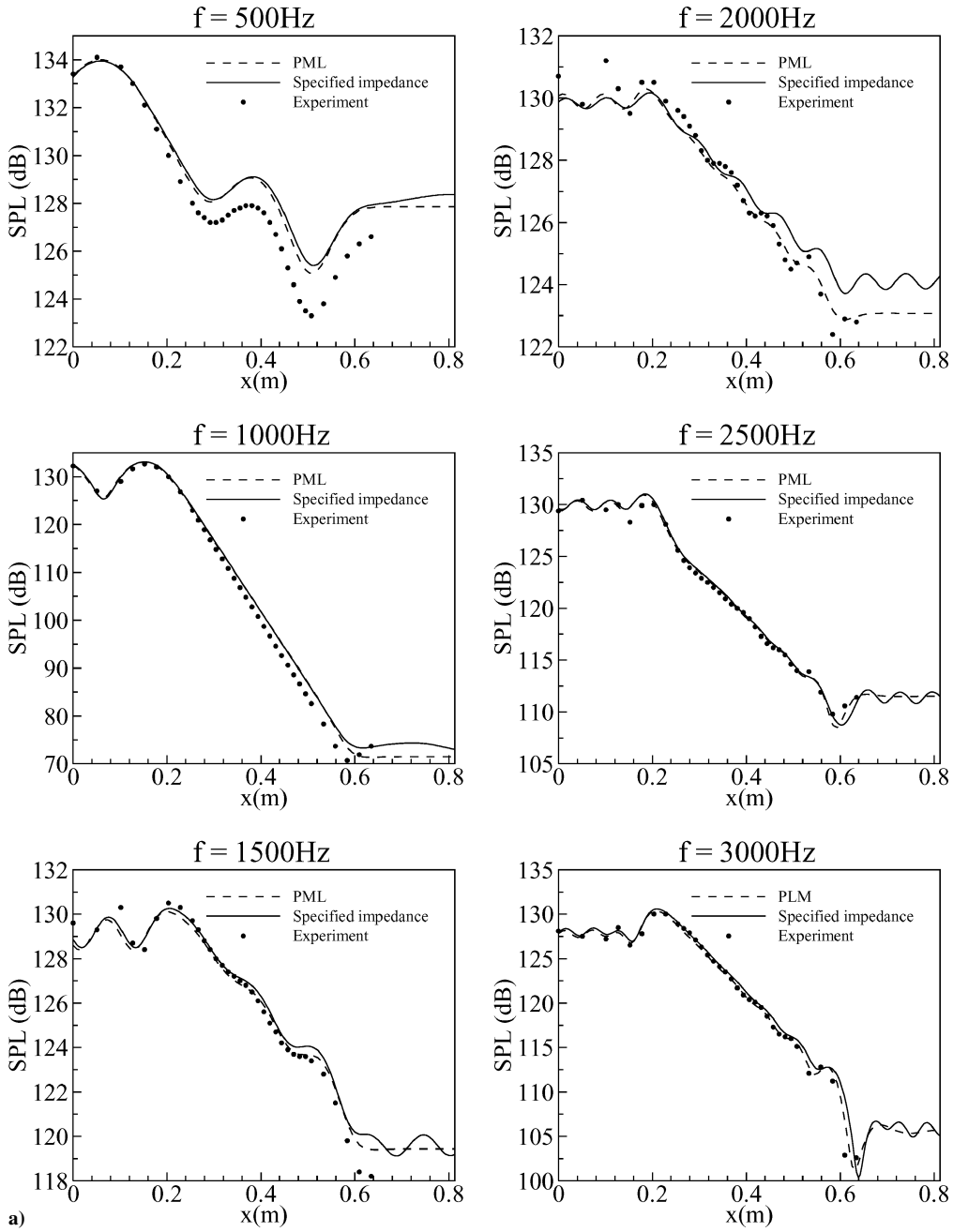

Fig. 5 Comparison of the numerical solution with the experimental result at test frequencies with a zero mean flow: a) SPL along the upper (hard) wall and b) phase along the upper (hard) wall.

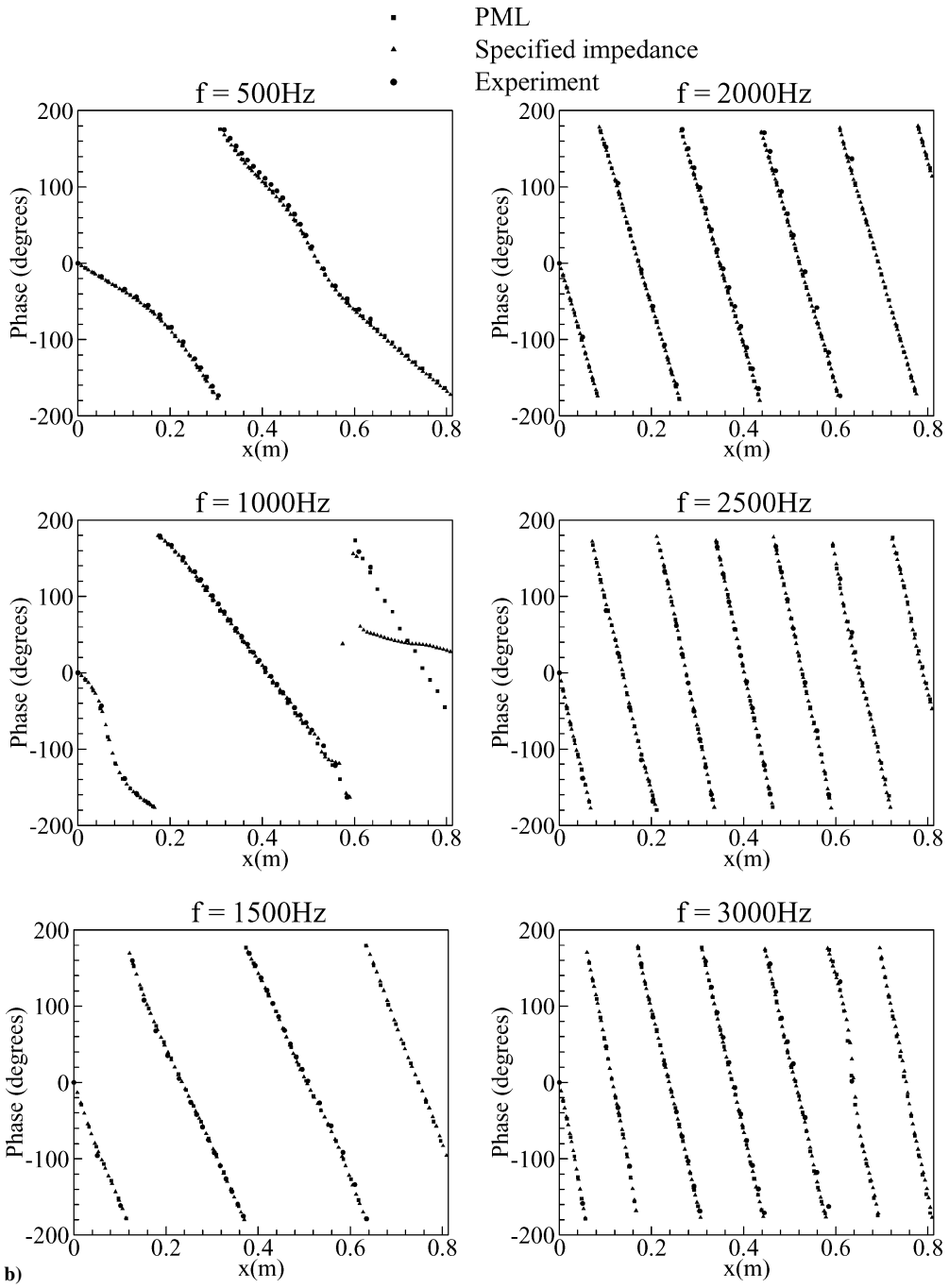

b)

Fig. 5 Comparison of the numerical solution with the experimental result at test frequencies with a zero mean flow: a) SPL along the upper (hard) wall and b) phase along the upper (hard) wall (continued).

can take an alternative approach that leads to the same result by using a stable no-slip time-domain impedance boundary condition and the fact that as the boundary-layer thickness approaches to zero the no-slip impedance boundary condition gives a limiting result of the combination of PDC and slip condition.[27,28]

3. Hard-Wall Boundary Condition

The hard-wall boundary condition is applied at the upper wall. A ghost point is introduced right above each of the node at the upper boundary in implementing the condition $\partial p/\partial y = 0$ at $y = h$. The hard wall can also be treated as a special case of the acoustically treated wall with $R(\omega) = X(\omega) = \infty$. In such a case, the adoption of either PDC or PVC does not make a difference, that is, Eqs. (6) and (7) are equivalent.

4. Numerical Scheme

The two-dimensional linearized Euler equations are numerically solved with a fourth-order seven-point-stencil optimized upwind dispersion-relation-preserving scheme.[29] The spatial coefficients for both the interior and the boundary points are the same as those listed in Ref. 29, whereas the temporal coefficients are from Ref. 30.

C. Comparison with the Analytical Solution

The semi-infinite impedance duct problem with only the least attenuated mode is used to test the numerical methods presented above. The domain of interest starts at $x = 0$ and ends at $x = 0.8382$, for which we use 216 grid points in the x direction and 14 grid points in the y direction with uniform spacings Δx and Δy. The PML boundary conditions with and without incoming waves are implemented in 10 vertical x layer left to $x = 0$ and 20 vertical x layers right to $x = 0.8382$. The time step is chosen such that CFL $= 0.05$ for Δx, where CFL is the Courant–Friedrichs–Lewy number. The parameters X_{-1} and X_1 for the reactance X are selected such that the specific impedance $Z = 4.99 + 0.25i$ is satisfied for the test frequency given earlier. We have conducted a grid-dependence study,

which shows that a converged solution is achieved with the preceding spatial and temporal resolutions. The calculation is started with all of the acoustic variables being zero everywhere in the computational domain and is terminated when the solution has become periodic. It takes about 90 s of CPU time and 1.2 MB of memory on a personal computer with an Athlon XP 1800+ CPU at 1533 MHz and 512-MB PC2100 DDR memory.

In Fig. 2, we compare the numerical solution with the analytical solution for the zero mean flow case. Shown in Fig. 2a is a comparison on the sound pressure level along the hard wall. It can be seen that the numerical solution coincides with the analytical solution described by a straight line very well even near the exit of the computational domain. Figure 2b compares the phase along the hard wall, where the phase is relative to the inlet point on the hard wall and has been converted into the range of [−180 deg, 180 deg]. Again, the agreement between the numerical solution and the analytical solution is excellent everywhere in the computational domain. Specially, the excellent agreements near the exit substantiate that the PML boundary condition indeed introduces little reflections.

With a sheared mean flow $M(y) = 1.2(y/h)(1 - y/h)$, the comparisons between the analytical and the numerical solutions are given in Fig. 3. As we can see, an excellent agreement between the two solutions is achieved.

By benchmarking our numerical methods with the analytical solution, we conclude that our numerical methods are accurate and reliable under the physical conditions and configurations in the test problem. In the next section, we are going to apply our numerical methods to the NASA impedance duct configuration.

III. Validation with Experimental Data

A. Experimental Setup

The experimental data from the Flow-Impedance Test Laboratory of NASA Langley Research Center[31] are used to validate our numerical methods. The duct configuration for the experiment is shown in Fig. 4, where acoustic treatment is applied only in the

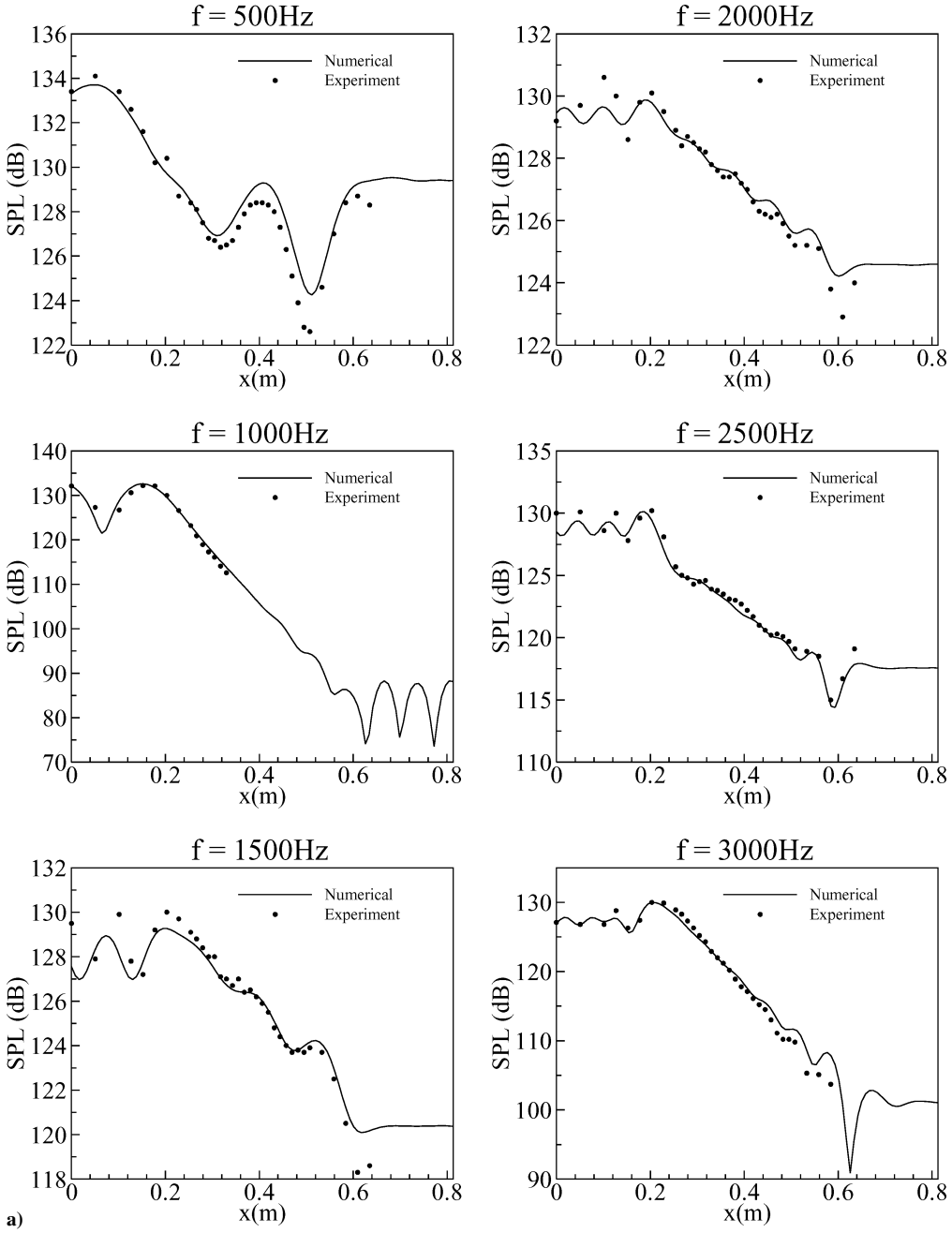

a)

Fig. 6 Comparison of the numerical solution with the experimental result at test frequencies with a mean flow profile assumed as $M(y) = 1.2(y/h)(1-y/h)$: a) SPL along the upper (hard) wall and b) phase along the upper (hard) wall.

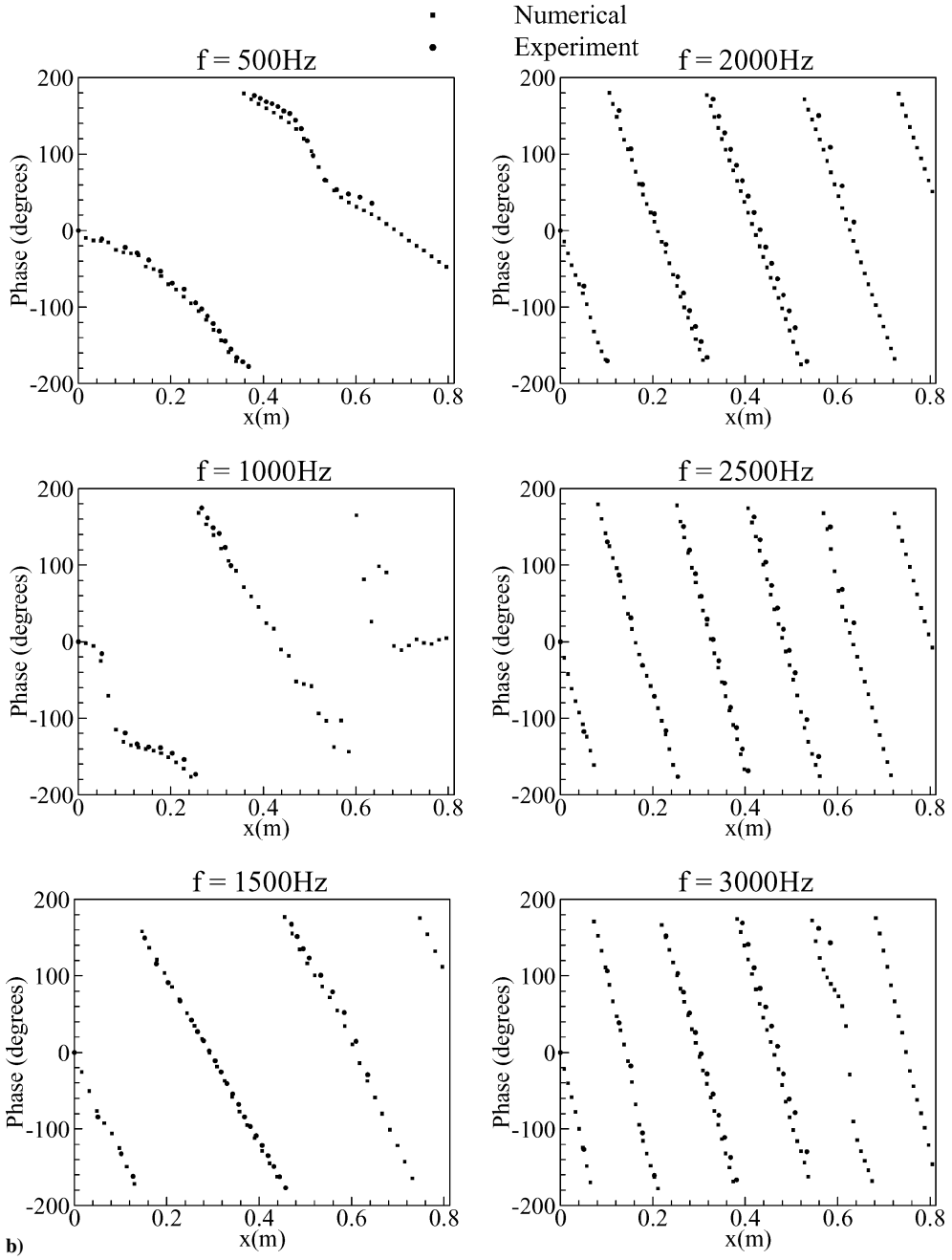

Fig. 6 Comparison of the numerical solution with the experimental result at test frequencies with a mean flow profile assumed as $M(y) = 1.2(y/h)(1-y/h)$: a) SPL along the upper (hard) wall and b) phase along the upper (hard) wall (continued).

middle section of the lower wall while all of the rest of the walls are hard wall. The liner impedance Z_{wall} and exit impedance Z_{exit} were experimentally measured at each test frequency $f = \omega/2\pi$ and are listed in Table 1. An incoming acoustic wave of each test frequency is supplied at the inlet, and its amplitude is adjusted such that the numerical result best matches the experimental data at the duct inlet for each test frequency.

Table 1 Impedance on the wall and at the exit

	Z_{wall}		Z_{exit}	
f, Hz	R	X	R	X
500	0.41	−1.56	1.077	0.008
1000	0.46	0.03	0.966	0.042
1500	1.08	1.38	0.935	−0.047
2000	4.99	0.25	1.094	−0.070
2500	1.26	−1.53	1.074	0.127
3000	0.69	−0.24	0.852	0.008

B. Numerical Results and Comparison with the Experimental Data

The NASA Langley flow-impedance tube problem is solved numerically by the numerical methods introduced in Sec. II.B. For the zero mean flow cases, both the PML boundary condition and the impedance boundary condition with the specified exit impedance Z_{exit} are considered for the exit boundary condition. The grid and time step used for both the cases are the same as for the verification problem except that for the latter case the vertical x layers right to the domain of interest are not needed, which correspondingly reduces the computational cost. The numerical results of SPL and the phase along the upper hard wall are shown in Fig. 5 for all of the test frequencies, where PML and specified impedance denote the boundary conditions used. As we can see, the agreements between the numerical results and the experimental measurements are in general very good. Note that when the PML boundary condition is used at the exit, there is virtually no reflection at the exit. The reflection is apparent when the specified impedance condition is used at the exit. However, because the reflection at the exit is small (small reflection coefficient) for all of the test frequencies the difference between

the numerical solutions with the two different boundary conditions at the exit is insignificant except for the case of 2000 Hz. For this case, there is a small discrepancy between the two numerical results. Figure 5 shows that the agreement between the numerical solution and the experimental data improves as the frequency increases. The reason for the improvement could be that the reflections at both the inlet and the exit are minimum at higher frequencies. Therefore the PML boundary conditions used are more adequate for these cases.

For the cases with a mean flow, only the PML boundary condition is applied at the exit. Because an accurate mean flow profile is not available, we assume the profile as $M(y) = 1.2(y/h)(1 - y/h)$ for the nominal Mach number 0.3. The same measured impedance parameters for the liner in Table 1 are used. The results are compared with the experimental data in Fig. 6. Again, the agreement between the numerical solution and the experimental data is very good for both the sound pressure level and the phase.

IV. Conclusions

A time-domain computational-aeroacoustics (CAA) code for duct acoustics is developed with a time-domain broadband impedance boundary condition. It is tested against the analytical solution of a semi-infinite impedance duct problem and the experimental data from the NASA Langley flow impedance tube facility in the presence of a sheared or zero mean flow. The results show that the CAA code can accurately predict duct acoustics in terms of both amplitude and phase.

We have tested only the numerical methods for single frequencies because both the analytical solution and the experimental data are available only for single-frequency cases. However, because the system of linearized Euler equations and the boundary conditions are linear, a series of tests at discrete frequencies representing the spectrum in a certain range should reasonably be equivalent to a broadband test in the same range. Because time-domain methods are able to handle broadband sound sources in one single simulation, the CAA code developed here can be used effectively as a noise prediction system for turbofan engine inlet ducts and turbomachinary. In addition, it can be used for impedance eduction when incorporated into an optimization process.

Acknowledgments

The work was partially supported by Grant NSF-MRSEC DMR09809688. We thank W. R. Watson at NASA Langley Research Center, Hampton, Virginia, for providing the experimental data and for his very helpful suggestions and comments.

References

[1]Eversman, W., Parrett, A. V., Preisser, J. S., and Silcox, R. J., "Contributions to the Finite Element Solution of the Fan Noise Radiation Problem," *Journal of Vibration, Acosutics, Stress and Reliability in Design*, Vol. 107, April 1985, pp. 216–223.

[2]Eversman, W., and Roy, I. D., "Ducted Fan Acoustic Radiation Including the Effects of Non-Uniform Mean Flow and Acoustic Treatment," AIAA Paper 1993-4424, Oct. 1993.

[3]Özyörük, Y., and Long, L. N., "Computation of Sound Radiating from an Engine Inlets," *AIAA Journal*, Vol. 34, No. 5, 1996, pp. 894–901.

[4]Rumsey, C. L., Biedron, R. T., Farassat, F., and Spence, P. L., "Duct-Fan Engine Acoustic Predictions Using a Navier–Stokes Code," *Journal of Sound and Vibration*, Vol. 213, No. 4, 1998, pp. 643–664.

[5]Stanescu, D., Ait-Ali-Yahia, D., Habashi, W. G., and Robichaud, M. P., "Multidomain Spectral Computations of Sound Radiation from Ducted Fans," *AIAA Journal*, Vol. 37, No. 3, 1999, pp. 296–302.

[6]Shim, I. B., Kim, J. W., and Lee, D. J., "Numerical Study on Radiation of Multiple Pure Tone Noise from an Aircraft Engine Inlet," AIAA Paper 99-1831, May 1999.

[7]Ahuja, V., Özyörük, Y., and Long, L. N., "Computational Simulations of Fore and Aft Radiation from Ducted Fans," AIAA Paper 2000-1943, June 2000.

[8]Nallasamy, M., Sutliff, D. L., and Heidelberg, L. J., "Propagation of Spinning Acoustic Modes in Turbofan Exhaust Ducts," *Journal of Propulsion and Power*, Vol. 16, No. 5, 2000, pp. 736–743.

[9]Rienstra, S. W., and Eversman, W., "A Numerical Comparison Between Multi-Scales and FEM Solution for Sound Propagation in Lined Flow Ducts," *Journal of Fluid Mechanics*, Vol. 437, 2001, pp. 367–384.

[10]Schoenwald, N., Schemel, C., Eschricht, D., Michel, U., and Thiele, F., "Numerical Simulation of Sound Propoagation and Radiation from Aero-Engine Intakes," *Proceedings of the 3rd Aeroacoustics Workshop (SWING)*, edited by S. Wagner and J. Ostertag, Dresden Univ. of Technology, Dresden, Germany, 2002.

[11]Li, X. D., Schoenwald, N., Yan, J., and Thiele, F., "A Numerical Study on Acoustic Radiation from a Scarfed Intake," AIAA Paper 2003-3245, May 2003.

[12]Zhang, X., Chen, X. X., Morfey, C. L., and Tester, B. J., "Computation of Fan Noise Radiation through a Realistic Engine Exhaust Geometry with Flow," AIAA Paper 2003-3267, May 2003.

[13]Zheng, S., and Zhuang, M., "Noise Prediction and Optimization System for Turbofan Engine Inlet Duct Design," AIAA Paper 2004-3031, May 2004.

[14]Li, X. D., Schemel, C., Michel, U., and Thiele, F., "Azimuthal Sound Mode Propagation in Axisymmetric Flow Ducts," *AIAA Journal*, Vol. 42, No. 10, 2004, pp. 2019–2027.

[15]Meyers, M. K., "On the Acoustic Boundary Condition in the Presence of Flow," *Journal of Sound and Vibration*, Vol. 71, No. 3, 1980, pp. 429–434.

[16]Motsinger, R. E., and Kraft, R. E., "Design and Performance of Duct Acoustic Treatment," *Aeroacoustics of Flight Vehicles: Theory and Practice*, NASA RP-1258, Aug. 1991, Chap. 14.

[17]Tam, C. K. W., and Auriault, L., "Time-Domain Impedance Boundary Conditions for Computational Aeroacoustics," *AIAA Journal*, Vol. 34, No. 5, 1996, pp. 917–923.

[18]Özyörük, Y., and Long, L. N., "A Time-Domain Implementation of Surface Acoustic Impedance Condition with and Without Flow," *Journal of Computational Acoustics*, Vol. 5, No. 3, 1997, pp. 277–296.

[19]Fung, K.-Y., and Ju, H., "Impedance and Its Time-Domain Extensions," *AIAA Journal*, Vol. 38, No. 1, 2000, pp. 30–38.

[20]Fung, K.-Y., and Ju, H., "Broadband Time-Domain Impedance Models," *AIAA Journal*, Vol. 39, No. 8, 2001, pp. 1449–1454.

[21]Özyörük, Y., Long, L. N., and Jones, M. G., "Time-Domain Numerical Simulation of a Flow-Impedance Tube," *Journal of Computational Physics*, Vol. 146, No. 1, 1998, pp. 29–57.

[22]Özyörük, Y., and Long, L. N., "Time-Domain Calculation of Sound Propagation in Lined Ducts with Sheared Flows," *AIAA Journal*, Vol. 38, No. 5, 2000, pp. 768–773.

[23]Ju, H., and Fung, K.-Y., "Time-Domain Impedance Boundary Conditions with Mean Flow Effects," *AIAA Journal*, Vol. 39, No. 9, 2001, pp. 1683–1690.

[24]Zheng, S., and Zhuang, M., "Three-Dimensional Benchmark Problem for Broadband Time-Domain Impedance Boundary Conditions," *AIAA Journal*, Vol. 42, No. 2, 2004, pp. 405–407.

[25]Tester, B. J., "The Propagation and Attenuation of Sound in Lined Ducts Containing Uniform of Plug Flow," *Journal of Sound and Vibration*, Vol. 28, No. 2, 1973, pp. 151–203.

[26]Hu, F. Q., "A Stable, Perfectly Matched Layer for Linearized Euler Equations in Unsplit Physical Variables," *Journal of Computational Physics*, Vol. 173, Nov. 2001, pp. 455–480.

[27]Tester, B. J., "Some Aspects of 'Sound' Attenuation in Lined Ducts Containing Inviscid Mean Flows with Boundary Layers," *Journal of Sound and Vibration*, Vol. 28, No. 2, 1973, pp. 217–245.

[28]Nayfeh, A. H., Kaiser, J. E., and Shaker, B. S., "Effect of Mean-Velocity Profile Shapes on Sound Transmission Through Two-Dimensional Ducts," *Journal of Sound and Vibration*, Vol. 34, No. 3, 1974, pp. 413–423.

[29]Zhuang, M., and Chen, R. F., "Applications of High-Order Optimized Upwind Schemes for Computational Aeroacoustics," *AIAA Journal*, Vol. 40, No. 3, 2002, pp. 443–449.

[30]Tam, C. K. W., and Webb, J. C., "Dispersion-Relation-Preserving Finite Difference Schemes for Computational Acoustics," *Journal of Computational Physics*, Vol. 107, No. 2, 1993, pp. 262–281.

[31]Parrott, T. L., Watson, W. R., and Jones, M. G., "Experimental Validation of a Two-Dimensional Shear Flow Model for Determining Acoustic Impedance," NASA TP-2679, May 1987.

D. Gaitonde
Associate Editor